J. Chem. Sci. (2023)135:7
https://doi.org/10.1007/s12039-022-02124-3

REGULAR ARTICLE

Thermoresponsive sustainable release of anticancer drugs using cyto-compatible pyrenylated hydrogel as vehicle

DIPEN BISWAKARMA[a,b], NILANJAN DEY[c] and SANTANU BHATTACHARYA[a,*]
[a]Department of Organic Chemistry, Indian Institute of Science, Bangalore 560012, India
[b]Solid State and Structural Chemistry Unit, Indian Institute of Science, Bangalore 560012, India
[c]Department of Chemistry, Birla Institute of Technology and Science Pilani, Hyderabad 500078, India
E-mail: sb@iisc.ac.in

MS received 9 September 2022; revised 5 December 2022; accepted 10 December 2022

Abstract. Pyrene-based fluorogenic amphiphilic probe (1) has been synthesized, which can form a thixotropic (injectable) hydrogel in the aqueous medium. The biocompatible hydrogel, so formed, is involved in the thermoresponsive, sustainable delivery of two anticancer drugs, Doxorubicin (DOX) and Mitoxantrone (MT). A substantial difference in the extent of drug release is noticed at 25 and 37 °C, even at physiological pH. The cumulative releases of ~80% and ~70% for DOX and MT, respectively, from the drug-loaded hydrogel samples, are observed for 72 h. In both cases, drug molecule release follows zero-order kinetics and non-Fickian diffusion pathways. The excellent stability of 1 against proteinase enzyme suggests that the present system can be used for sustainable, targeted release of drug molecules under in-vivo conditions. As expected, DOX-loaded hydrogels kill cancer cells more efficiently than the free drug (i.e., DOX).

Keywords. Thixotropic behavior; Thermoresponsiveness; Sustainable delivery; Drug-loaded hydrogel; *Cyto-compatibility*.

1. Introduction

Stimuli-sensitive hydrogels have recently received a significant public attraction as they offer incredibly diversified applications, including their use as catalytical reactions,[1] actuator,[2] and sensors[3] for biomedical applications such as drug delivery systems,[4] diagnostics,[5] cancer therapy,[6] regenerative medicine,[7] etc. Drug delivery involving polymer-based hydrogels has been used over the last decade because of their swelling properties.[8] Since the maximum volume of the micropores in the hydrogel is filled with water, they can entrap the bioactive molecules inside its matrix and then release them through diffusion or by the degradation of the hydrogel. It has often been observed that exposure of hydrogels to different stimuli, namely light, pH, temperature, redox, external stress, and biomolecules, can result in gel-to-sol transition and subsequent release of drug molecules.[9–11] For instance, Zhu and co-workers have reported pH-responsive drug delivery using a sugar-appended hydrogelator with an aldehyde group.[12] Similarly, Zhang *et al.,* demonstrated the release of drug molecules from an azobenzene-based hydrogel system upon light irradiation.[13] On the other hand, Feng and co-workers have shown redox-controlled release of drug molecules by disrupting disulfide bonds.[14]

Among LMWGs, carbohydrate-based hydrogels have shown promising applications as responsive biomaterials because they not only provide intensely chiral hydrophilic building blocks with high water solubility but are often also biocompatible and biodegradable.[16] Moreover, carbohydrates with cyclic forms contain multiple and directional hydroxyl groups, which can support the self-assembled organization by forming significant hydrogen-bonding networks.[17,18] Considering these, we have explored the self-assembly and drug delivery properties of a pyrene-based fluorogenic amphiphile with disaccharide (lactose, **1**) as a hydrophilic unit. The self-assembly properties of **1** hydrogel were probed using various

*For correspondence
Supplementary Information: The online version contains supplementary material available at https://doi.org/10.1007/s12039-022-02124-3.

Published online: 18 January 2023

spectroscopic and microscopic techniques, showing the formation of vesicular nano-aggregates. The hydrogel was then exploited towards thermoresponsive sustainable delivery of two clinically used anticancer drugs, such as Doxorubicin and Mitoxantrone, under physiological conditions (pH 7.4 buffer medium).

2. Experimental

2.1 *Material and methods*

All chemicals, solvents, chemicals, and silica gel for TLC were obtained from best-known commercial sources and were used without further purification. Solvents were distilled and dried before use. Melting points were measured in open capillaries and were uncorrected. ^{1}H-NMR and ^{13}C-NMR spectra were recorded in Bruker-400 Advance NMR spectrometer. The internal standard tetramethyl silane (TMS) reported chemical shifts in ppm downfield. Mass spectrometry of individual compounds was performed using a Micro Mass ESI-TOF MS instrument. Elemental analysis was recorded in Thermo Finnigan EA FLASH 1112 SERIES.

2.2 *Gelation studies*

The formation of the gel was confirmed using the tube inversion method. If a gel was formed, it was evaluated quantitatively by determining the critical gelator concentration (CGC) and the minimum amount of gelator required to immobilize 1 mL of a solvent or solvent mixture. A glass tube with 10 x 75 mm capacity has been used for CGC measurement.

2.3 *Fluorescence spectroscopy*

The fluorescence spectra were recorded on a Cary-Eclipse spectrofluorimeter equipped with a temperature controller bath. For the fluorescence experiment, the slit width for the excitation and emission channel was fixed at 5 nm. The excitation wavelength was considered 370 nm for all spectroscopic studies.

2.4 *Fluorescence microscopy*

A diluted solution of **1** was drop cast on a cleaned glass slide, left overnight for drying in a dust-free environment, and finally evacuated. The microscopic fluorescence images were taken on an Olympus IX-71 microscope with 300-400 nm UV light excitation.

2.5 *Dynamic light scattering (DLS)*

DLS measurements were performed at room temperature using a Malvern Zetasizer Nano ZS particle sizer (Malvern Instruments Inc., Westborough, MA). Samples were prepared and examined under dust-free conditions. Average hydrodynamic diameters (Dh) reported were obtained from the Gaussian analysis of the intensity-weighted particle size distributions.

2.6 *Drug encapsulation*

An aqueous solution of the DOX/MT (50 μg/mL) was added from a stock solution (2 mg/mL) to the fleshly prepared hydrogel (2.5 mM). The drug-loaded hydrogel was then sonicated and kept at rest for 5 mins. After five minutes, we observed the formation of stable gel, which was then used for the release study.

2.7 *Drug release study*

To the fleshly prepared drug-encapsulated hydrogel, 1 mL of PBS buffer (10 mM) of pH 7.4 was added and incubated at 37 °C. The supernatant layer was removed and taken from DOX/MT encapsulated hydrogel on incubation, and then UV-visible spectra were recorded. After recording the absorption spectra, the solution was again added back to the drug-encapsulated hydrogel gradually, and this process was continued for several hours. This method was utilized to quantify the number of drugs released from the gel matrix.

2.8 *Cell culture*

HeLa cells were cultured in Dulbecco's Modified Eagle's Medium (DMEM, CELL clone, India) containing 10% FBS (Invitrogen, USA) and antibiotics (100 units/mL penicillin and 100 μg/mL streptomycin). Cells were incubated in a humidified 5% CO_2 incubator (Sanyo, UK) at 37 °C.

2.9 *Cell viability assay*

Cytotoxicity of the **1**, was evaluated in HeLa cells by the 3-(4,5-dimethylthiazol-2-yl)-2,5- diphenyltetrazolium bromide (MTT) assay. In a typical experiment,

cells were seeded at a density of ~1 × 104 cells/well in the 96 well plates and incubated for 24 h. Then, the cells were treated with different concentrations of the probe. Finally, cells were washed, and 20 µL of MTT (5 mg/mL in DMEM) was added to each well and incubated for 3 h in the dark. Finally, the whole medium was removed from the wells, and DMSO (100 µL) was added. The cells were incubated for 5 min in the dark, and absorbance was measured at 560 nm. Similarly, cell viability assays with different DOX: **1** composite were performed following the same procedure.

3. Results and Discussions

3.1 *Design and Synthesis of gelator molecule*

The sugar-appended pyrenyl amphiphile (Figure 1a), Compound **1,** was synthesized following a procedure reported in the literature.[15] In a typical experiment, **1** was prepared by refluxing 1-pyrene butyric acid hydrazine derivative with lactose in MeOH/$CHCl_3$ (3:1 v/v) medium for 36 h without involving any protection or deprotection step. The chemical structure of **1** was characterized using ^{1}H-NMR, ^{13}C-NMR, FT-IR, ESI-MS, and elemental analysis.

3.2 *Suitability of hydrogel system as a delivery vehicle*

The hydrogel formed (CGC: 1.3 mM) was found to be thermoreversible, as confirmed by repetitive freeze-thaw cycles. Moreover, vesicular hydrogel samples (Figure 1c, 1d) remained stable over an extended period without decomposition. These two properties are essential to designing sustainable, thermoresponsive delivery systems. Furthermore, the hydrogel rapidly converted to sol under mechanical stress but reverted to gel upon resting, indicating the hydrogel's thixotropic property (Figure 1f). The main advantages of the thixotropic hydrogels are that they possess shear-thinning properties, which means that they can flow as sol under the required shear stress during injection using a syringe and revert to solid-like gel on cessation of that applied stress (Figure 1b). Recently, injectable hydrogels have received enormous public attention, especially as drug delivery vehicles, because of their unique properties, including pharmacokinetic behavior.[19] These abilities of the 'injectable' hydrogel to undergo facile sol-to-gel transition have indeed been utilized as a viable candidate for biomedical application, especially for encapsulation and the sustainable release of bioactive molecules. Moreover, injectable hydrogels are more efficient than traditional

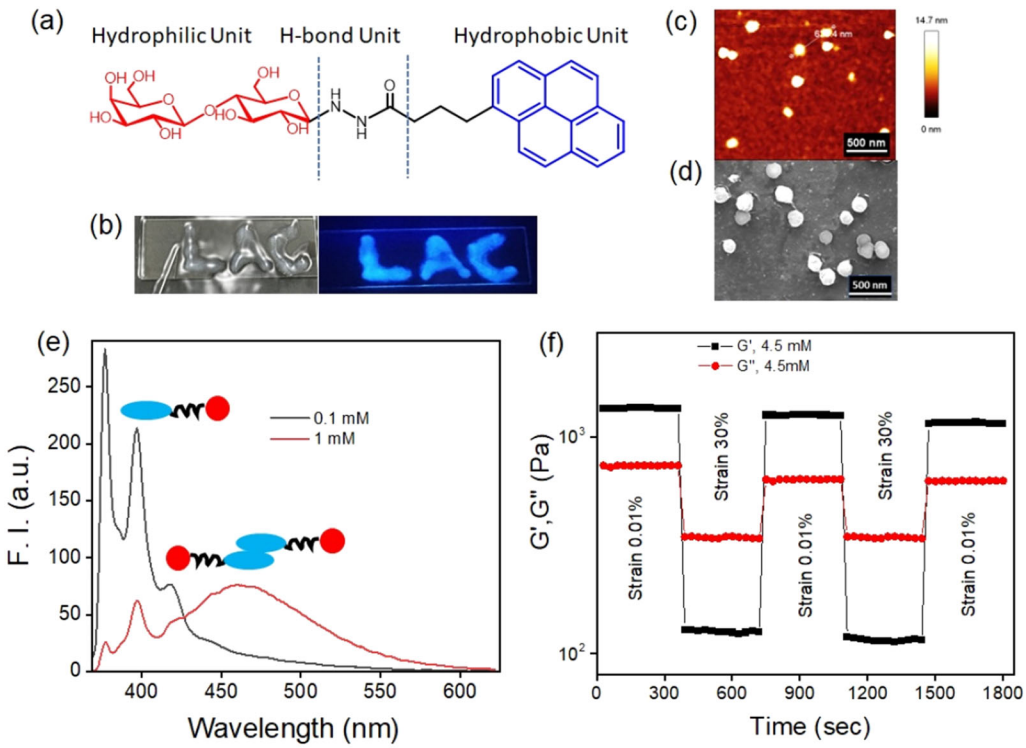

Figure 1. (a) Structure of **1** amphiphile. (b) Injectability property of hydrogel of **1** (under daylight and the long UV- Lamp > the 360 nm) (c) AFM and (d) SEM images of the hydrogel of **1** (0.10 mM). (e) Emission spectra of **1** at low and high concentrations (λ_{ex} = 345 nm) in water. (f) Hysteresis loop test rheology data of hydrogel of **1** (4.5 mM).

hydrogels since the bioactive material may be administered non-invasive and simply.[20,21]

The fluorescence spectra of the compound showed two vibronic peaks at 378 nm and 396 nm attributed to monomeric pyrene units of **1** (Figure 1e). Broadband was observed at 470 nm, presumably due to π-stacked aggregates of pyrene moieties.[22] The variable temperature emission studies showed enhancement in the monomer emission with increasing temperature (20 to 65 °C) at the expense of aggregate emission (Figure S1, SI). This indicates a 'slipped' π-π stacking structure due to thermal agitation at elevated temperatures.[23] However, the reappearance of aggregate emission at 470 nm could be traced when the same solution was cooled down (thermoreversible). These results indicate that the monomer and aggregates forms of **1** remain in equilibrium at biological pH, and heat can shift the balance in the desired direction.

3.3 *Loading of drug molecules into the hydrogel matrix*

It is well known that injectable hydrogels are considered a unique tool in biomedical applications, especially for drug delivery. Accordingly, we also explored our injectable hydrogel as a drug delivery system for releasing anticancer drugs, e.g., Doxorubicin (DOX) and Mitoxantrone (MT). Both DOX and MT were encapsulated by physically entrapping them as a solution during the hydrogel formation. In a typical encapsulation process, the requisite amount of the drug in an aqueous solution (50 μg/mL) was mixed with the solution of **1** (2.5 mM) at 25 °C.[24] The resultant mixture was then sonicated, then cooled to room temperature. We observed that within 2 min, it formed a stable gel even in the drug's presence, indicating its facile encapsulation (Figure 2a). Encapsulation of the DOX can also be observed from the fluorescence microscopy image because of the presence of a hydrophobic environment, where DOX becomes more fluorescent, and the DOX release from the hydrogel matrix to bulk water is also evident from images (Figure 2b). Also, we observed high anisotropy values for the drug molecules upon encapsulation (Figure 2c). This is presumably due to the conformational restriction of drug molecules in the hydrogel matrix.[25]

The injectable ability of the hydrogels in both cases was tested by pulling the drug-doped hydrogel through a 21-gauge syringe and injecting them back into the gelation tube; within one minute, it reverted to a gel. After confirming the encapsulation of the drug, we then investigated the release of these drugs from the hydrogel matrix (Figure 2a).

3.4 *Thermoresponsive sustainable release of drug molecules*

The encapsulated drug's release profile was investigated by adding the buffer (pH= 7.4) on top of the DOX/MT loaded hydrogel, followed by incubation at 37 °C. The time-dependent drug release was then examined by recording the absorbance of the supernatant solution from time to time at 485 nm for DOX and 608 nm for Mitoxantrone, respectively (Figure 3a, b). The color (red for the DOX-doped hydrogel and blue for the MT-doped hydrogel) of the upper aqueous layers intensified with time while the gel parts continually turned pale. This essentially indicates the time-dependent sustainable release of the drug molecules from the gel matrix at 37 °C temperature. The release profile of both DOX and MT from the hybrid hydrogel system was bimodal, with an initial burst phase [0-30 h for DOX and 0-25 h for MT] followed by the sustained release of drugs over the next 72 h.[24] Figures 3c and 3d indicate the cumulative release of ~80% and ~70% for DOX and MT, respectively, from the drug-loaded hydrogel samples at 37 °C. However, in both cases, the release kinetics was substantially slow at 25 °C. The observation suggests that temperature plays a vital role in the release of drugs from the hybrid hydrogel sample. This is presumably because temperature induces disruption of the self-assembled structure, which results in the initial burst release of the drug molecules from the hydrophobic interior of the hydrogel network.

The kinetics of the drug's release from the hydrogel matrix was studied by fitting them into the kinetic equation (equation i) as cumulative % release vs. time, as shown below.

$$C = K_0 t \quad \text{(i)}$$

Where, k_0 = zero-order rate constant expressed in units of concentration/time, t = time in h.

It is worth mentioning that the release of both the drugs obeys the zero-order kinetics as we observed the burst release initially (Figure 4a) and then slow release after that [0-30 h for DOX and 0-25 h for MT].[25] The mechanism of the release was also examined (fitting into Peppa's model) by plotting (equation ii) log cumulative % versus log time, and exponential release component (n) was calculated from the slope of the straight line.

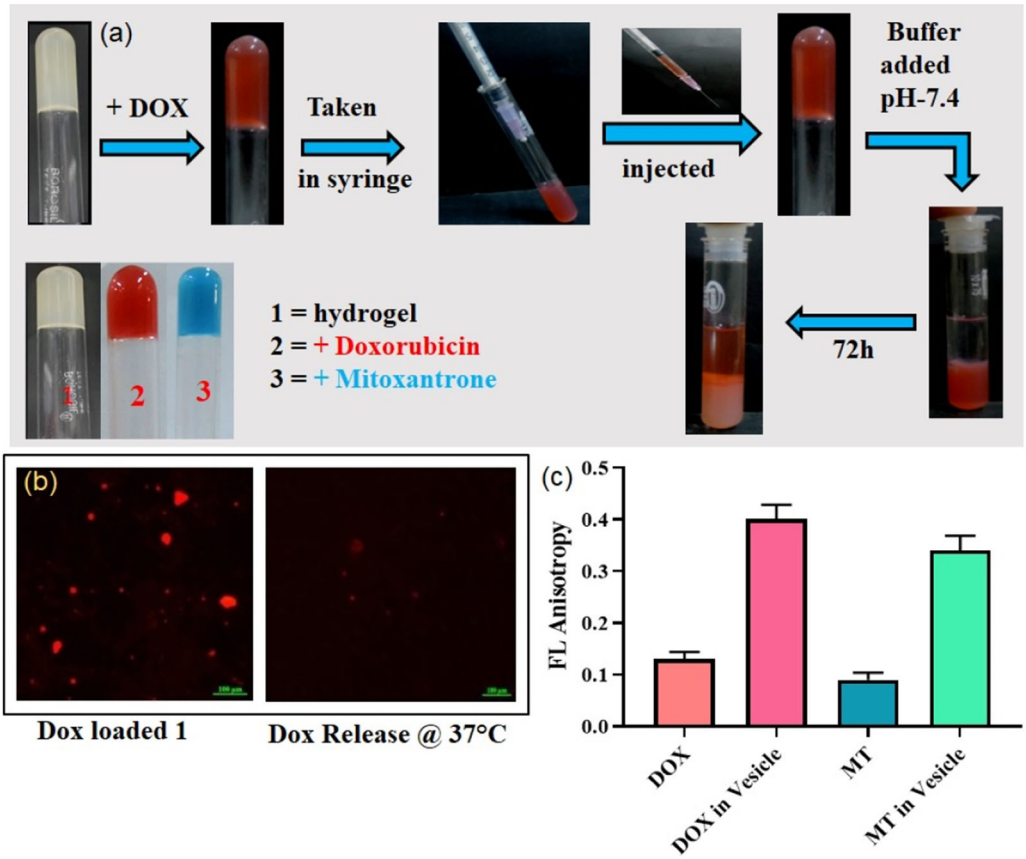

Figure 2. (a) Picture of DOX and MT encapsulated hydrogel of **1**, and the schematic shows the release of DOX at 37 °C, pH 7.4. (b) Fluorescence microscopic images of DOX encapsulated hydrogel of **1** (right side image shows DOX-loaded hydrogel and left image shows DOX release @ 37 °C). (c) Fluorescence anisotropies of DOX and MT in hydrogel matrix of **1**.

$$M_t/M_f = b * t^n \quad \text{(ii)}$$

Where M_t = amount of drug release at time t, M_f = overall amount of the drug, b = constant, and n = release exponent indicative of the drug release mechanism.

It was observed that the value of n was nearly 1 for both DOX/MT encapsulated hydrogel. Hence the present systems appear to follow the non-Fickian diffusion pathway (Figure 4b).[26]

3.5 *Cyto-compatibility of hydrogel for sustainable delivery*

For practical, sustainable drug delivery (Figure 4c), it is essential to check the Cyto-compatibility of the amphiphilic probe. Thus, the cytotoxicity of **1** was assayed against HeLa cells (cervical cancer cells) using MTT (3-(4,5-dimethylthiazol-2-yl)-2,5-diphenyl tetrazolium bromide) as the indicator dye.[27] Fortunately, no considerable reduction in the cell viability was noticed even when the cells were incubated with ~50 μM of the compound for more than 48 h (Figure 5a). This observation ensured that the probe could safely be used as a drug delivery vehicle for *in vivo* applications. Also, for effective delivery, the hydrogel microparticles need to remain stable in the bloodstream and shouldn't be degraded by protease enzymes before reaching the target location. To check this, we investigated the stability of the gelator molecules in the presence of the proteinase K enzyme.[24] In a typical experiment, **1** was incubated with proteolytic enzyme proteinase K in HEPES buffer at 25 °C for 24 h. The extent of enzymatic degradation was monitored by recording mass spectrum data at different intervals. No change in mass spectral analysis corresponding to the molecular ion peak $(M + H)^+$ to the time confirms that **1** is resistant to proteolysis (Figure 5b). Such proteolytic stability of the gelator molecules indicates that hydrogel discussed here can be used for the sustained release of drugs and essential biomolecules under physiological conditions.

Further, we also observed that Doxorubicin-loaded hydrogels kill cancer cells more efficiently than the free drug (*i.e.*, Doxorubicin).[28] Interestingly,

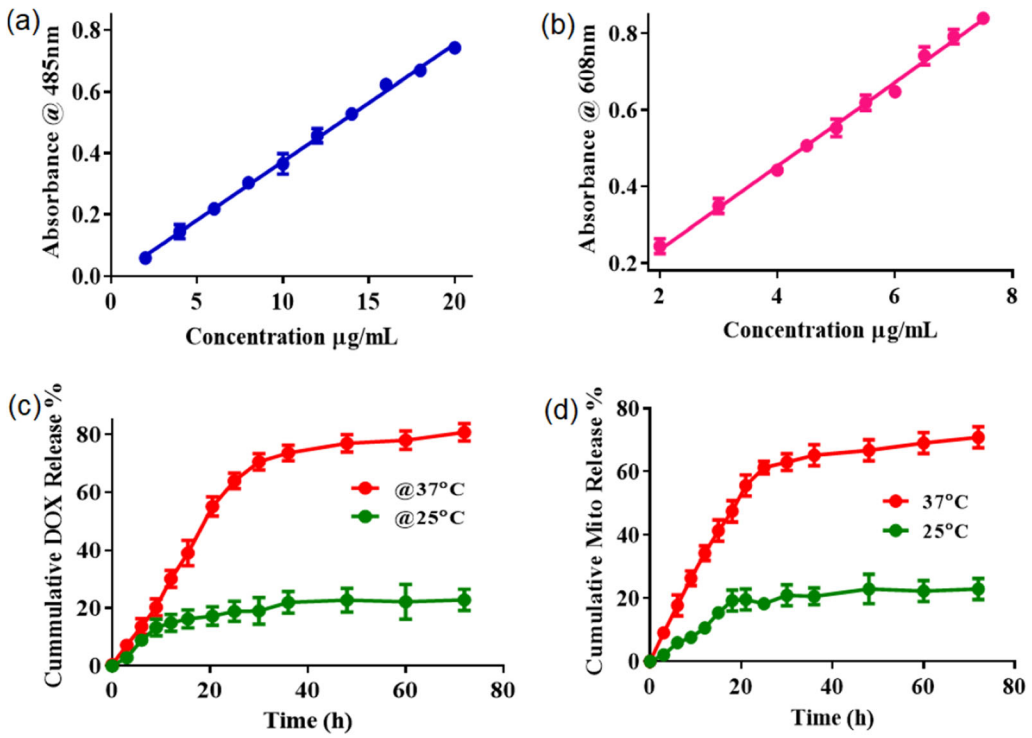

Figure 3. Standard plots show absorbance changes upon loading (a) DOX and (b) MT in the hydrogel of **1** matrix. Cumulative release profile of (c) DOX (50 µg/mL), (d) MT (50 µg/mL) loaded hydrogel (2.5 mM) at pH 7.4 at 37 °C and 25 °C, respectively.

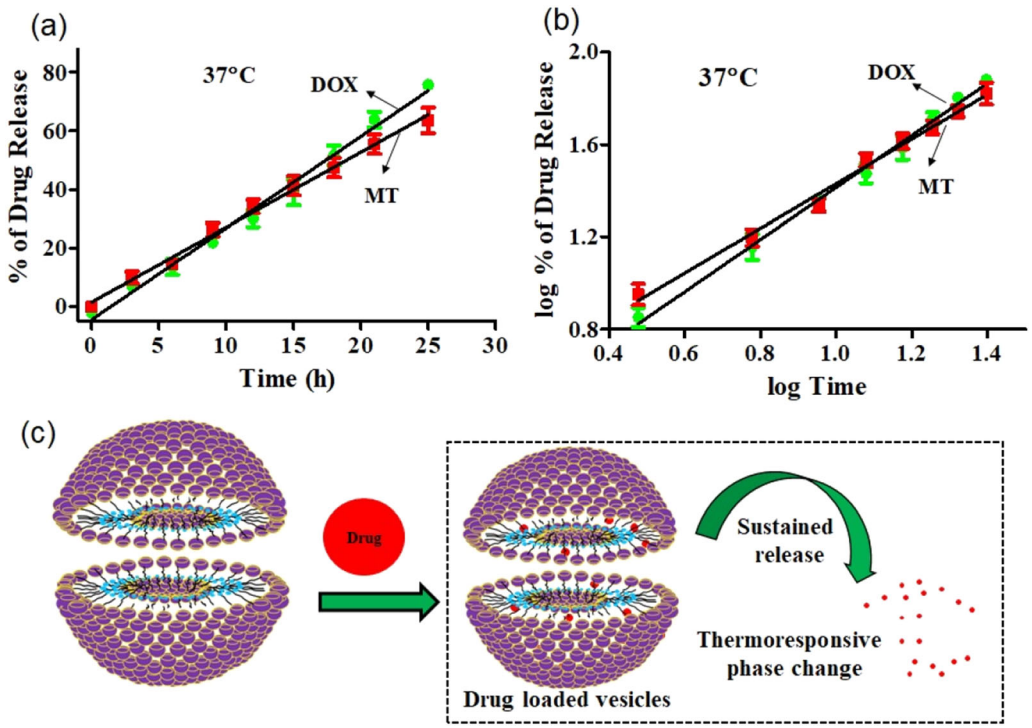

Figure 4. (a) Fitting of initial DOX (50 µg/mL) and MT (50 µg/mL) released from hydrogel of **1** (2.5 mM) to zero-order kinetics at pH 7.4, 37 °C. (b) Peppa's Kinetic model for DOX (50 µg/mL) and MT (50 µg/mL) released from the hydrogel of **1** (2.5 mM) at pH 7.4, 37 °C (c) Schematic diagram shows the temperature-induced release of encapsulated drug molecules from hydrogel matrix of **1**.

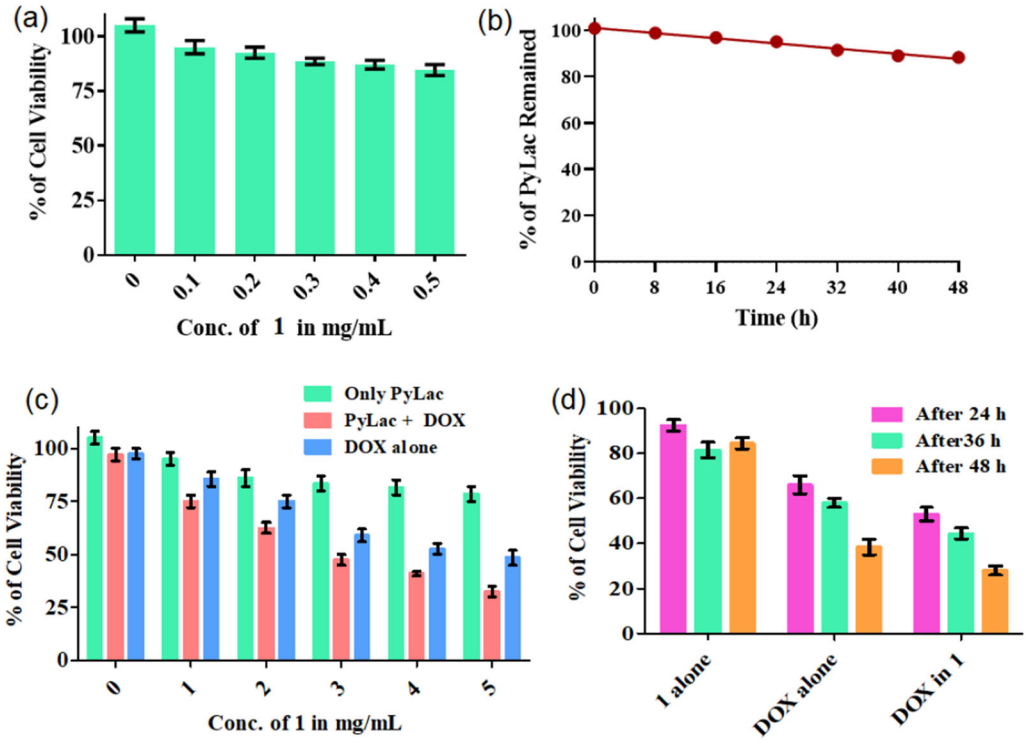

Figure 5. (a) Cytotoxic effects of **1** on HeLa cells as evaluated by MTT assay. (b) Proteolytic stability of **1** against proteinase K enzyme. (c) Cell viability assay with DOX-loaded **1** hydrogel at different doses of **1**. (d) Cell viability assay with DOX-loaded **1** hydrogel at different periods.

increasing gelator concentration (maintaining the same ratio for **1**: Dox) enhanced the extent of cell death (Figure 5c). Since the gelator molecule was biocompatible, we might expect that increase in cell death might be attributed to improved cellular internalization of drug molecules. This indicates the suitability of **1** as a delivery vehicle for anticancer drugs. Also, the cells were exposed to Doxorubicin-loaded hydrogels for 24, 36, and 48 h (Figure 5d). As expected, the extent of cell death was found to be maximum (∼ 75%) after 48 h.

4. Conclusions

In conclusion, we have developed a thixotropic injectable hydrogel system based on a pyrene-disaccharide conjugate, **1**. A detailed spectroscopic study and morphological analysis indicate the formation of thermoreversible vesicular nano-aggregates. Injectable and thixotropic properties of the hydrogels allowed the entrapping of the anticancer drug, namely Doxorubicin and Mitoxantrone, in the gel matrix, followed by their temperature-sensitive sustainable release at physiological pH. The release profiles show zero-order kinetics, and the pathway for the release of drugs from the gel matrix was found to be a non-Fickian diffusion pathway. Finally, the cytocompatibility of **1** hydrogel and good stability against the proteinase enzyme suggests that the present system can be used for sustainable, targeted release of drug molecules under physiological conditions. Further, it was observed that drug-loaded hydrogels kill cancer cells more efficiently than free drugs. This might be attributed to improved cellular internalization of drug molecules, which indicates the suitability of **1** as a delivery vehicle for anticancer drugs.

Supplementary Information (SI)

The supplementary information file contains the synthesis and characterization of compound **1** and ^{1}H-NMR and ^{13}C-NMR spectrum of compound **1**. The supplementary information is available at www.ias.ac.in/chemsci.

Acknowledgments

Prof. S. Bhattacharya thanks the Department of Science and Technology for the J. C. Bose Fellowship. D. Biswakarma thanks DSKPDF for funding.

Author contributions SB designed the project; DB and ND did experimental findings and data collection. DB prepared the original manuscript draft, and DB, ND, and SB did review and editing.

References

1. Díaz D D, Kühbecka D and Koopmans R J 2011 Stimuli-responsive gels as reaction vessels and reusable catalysts *Chem. Soc. Rev.* **40** 427
2. Shi Q, Liu H, Tang D, Li Y, Li X J and Xu F 2019 Bioactuators based on stimulus-responsive hydrogels and their emerging biomedical applications *NPG Asia Mater.* **11** 64
3. Biswakarma D, Dey N and Bhattacharya S 2022 A biocompatible hydrogel as a template for oxidative decomposition reactions: a chemodosimetric analysis and in vitro imaging of hypochlorite *Chem. Sci.* **13** 2286
4. Pourjavadi A, Heydarpour R and Tehrani Z M 2021 Multi-stimuli-responsive hydrogels and their medical applications *New J. Chem.* **45** 15705
5. Sood N, Bhardwaj A, Mehta S and Mehta A 2016 Stimuli-responsive hydrogels in drug delivery and tissue engineering *Drug Deliv.* **23** 748
6. Andrade F, Roca-Melendres M M, Durán-Lara E F, Rafael D and Jr. S S 2021 Stimuli-Responsive Hydrogels for Cancer Treatment: The Role of pH, Light, Ionic Strength and Magnetic Field *Cancers* **13** 1164
7. Li Z, Zhou Y, Li T, Zhang J and Tian H 2022 Stimuli-responsive hydrogels: Fabrication and biomedical applications *View* **3** 20200112
8. Narayanaswamy R and Torchilin V P 2019 Hydrogels and Their Applications in Targeted *Drug Deliv. Mol.* **24** 603
9. Shen Z, Guo Z, Tan T, Hu J and Zhang Y 2020 Reactive Oxygen Species Scavenging and Biodegradable Peptide Hydrogel as 3D Culture Scaffold for Cardiomyocytes *ACS Biomater. Sci. Eng.* **6** 3957
10. Biswakarma D, Dey N and Bhattacharya S 2020 A two-component charge transfer hydrogel with excellent sensitivity towards the microenvironment: a responsive platform for biogenic thiols *Soft Matter.* **16** 9882
11. Panda J J, Mishra A, Basu A and Chauhan V S 2008 Stimuli Responsive Self-Assembled Hydrogel of a Low Molecular Weight Free Dipeptide with Potential for Tunable Drug Delivery *Biomacromolecules* **9** 2244
12. Zhu Y-J and Chen F 2015 pH-Responsive Drug-Delivery Systems *Chem. Asian J.* **10** 284
13. (a) Huang Y, Qiu Z, Xu Y, Shi J, Lina H and Zhang Y 2011 Supramolecular hydrogels based on short peptides linked with conformational switch *Org. Biomol. Chem.* **9** 2149; (b) Srivastava A, Ghorai S, Bhattacharjya A and Bhattacharya S 2005 A tetrameric sugar-based azobenzene that gels water at various pH values and in the presence of salts *J. Org. Chem.* **70** 6574
14. Ji W, Liu G F, Xu M X and Feng C L 2015 A Redox-Responsive Supramolecular Hydrogel for Controllable Dye Release *Macromol. Chem. Phys.* **216** 1945
15. Biswakarma D, Dey N and Bhattacharya S 2020 A thermo-responsive supramolecular hydrogel that senses cholera toxin via color-changing response *Chem. Commun.* **56** 7789
16. Pramanik B, Singha N and Das D 2019 Sol-, Gel-, and Paper-Based Detection of Picric Acid at Femtogram Level by a Short Peptide Gelator *ACS Appl. Polym. Mater.* **1** 833
17. Dutta S and Bhattacharya S 2015 Multifarious facets of sugar-derived molecular gels: molecular features, mechanisms of self-assembly and emerging applications *Chem. Soc. Rev.* **44** 5596
18. Biswakarma D, Dey N and Bhattacharya S 2022 Molecular design of amphiphiles for Microenvironment-Sensitive kinetically controlled gelation and their utility in probing alcohol contents *J. Colloid Interface Sci.* **615** 335
19. Pertici V, Pin-Barre C, Rivera C, Pellegrino C, Laurin J, Gigmes D and Trimaille T 2019 Degradable and Injectable Hydrogel for Drug Delivery in Soft Tissues *Biomacromolecules* **20** 149
20. Xiong L, Luo Q, Wang Y, Li X, Shena Z and Zhu W 2015 An injectable drug-loaded hydrogel based on a supramolecular polymeric prodrug *Chem. Commun.* **51** 14644
21. Moon H J, Ko D Y, Park M H, Joo M K and Jeong B M 2012 Temperature-responsive compounds as in situ gelling biomedical materials *Chem. Soc. Rev.* **41** 4860
22. Hoche J, Schmitt H C, Humeniuk A, Fischer I, Mitric R and Rohr M I S 2017 The mechanism of excimer formation: an experimental and theoretical study on the pyrene dimer *Phys. Chem. Chem. Phys.* **219** 25002
23. Yan N, Xu Z, Diehn K K, Raghavan S R, Fang Y and Weiss R G 2013 How Do Liquid Mixtures Solubize Insoluble Gelators? Self-Assembly Properties of Pyrenyl-Linker-Glucono Gelators in Tetrahydrofuran-Water Mixtures *J. Am. Chem. Soc.* **135** 8989
24. Basu K, Baral A, Basak S, Dehsorkhi A, Nanda J, Bhunia D, *et al*. 2016 Peptide based hydrogels for cancer drug release: modulation of stiffness, drug release and proteolytic stability of hydrogels by incorporating d-amino acid residue(s) *Chem. Commun.* **52** 5045
25. Moitra P, Kumar K, Kondaiah P and Bhattacharya S 2014 Efficacious Anticancer Drug Delivery Mediated by a pH-Sensitive Self-Assembly of a Conserved Tripeptide Derived from Tyrosine Kinase NGF Receptor *Angew. Chem. Int. Ed.* **53** 1113
26. Sanson C, Schatz C, Le Meins J-F, Soum A, Thévenot J, Garanger E and Lecommandoux S 2010 A simple method to achieve high doxorubicin loading in biodegradable polymersomes *J. Control. Release* **147** 428
27. Dey N, Ali A, Mohini K and Bhattacharya S 2019 Simultaneous sensing of ferritin and apoferritin proteins using an iron-responsive dye and evaluation of physiological parameters associated with serum iron estimation *J. Mater. Chem. B* **7** 986
28. Singh M, Kundu S, Reddy M A, Sreekanth V, Motiani R K, Sengupta S, *et al*. 2014 Injectable small molecule hydrogel as a potential nanocarrier for localized and sustained in vivo delivery of doxorubicin *Nanoscale* **6** 12849